



CHALMERS

Chalmers Publication Library

Multi-level characteristic basis function method (MLCBFM) for the analysis of large antenna arrays

This document has been downloaded from Chalmers Publication Library (CPL). It is the author's version of a work that was accepted for publication in:

Radio Science Bulletin (ISSN: 1024-4530)

Citation for the published paper:

Maaskant, R. ; Mittra, R. ; Tijhuis, A. (2011) "Multi-level characteristic basis function method (MLCBFM) for the analysis of large antenna arrays". Radio Science Bulletin, vol. 336(3), pp. 23-34.

Downloaded from: <http://publications.lib.chalmers.se/publication/154324>

Notice: Changes introduced as a result of publishing processes such as copy-editing and formatting may not be reflected in this document. For a definitive version of this work, please refer to the published source. Please note that access to the published version might require a subscription.

Chalmers Publication Library (CPL) offers the possibility of retrieving research publications produced at Chalmers University of Technology. It covers all types of publications: articles, dissertations, licentiate theses, masters theses, conference papers, reports etc. Since 2006 it is the official tool for Chalmers official publication statistics. To ensure that Chalmers research results are disseminated as widely as possible, an Open Access Policy has been adopted. The CPL service is administrated and maintained by Chalmers Library.

Multilevel Characteristic Basis Function Method (MLCBFM) for the Analysis of Large Antenna Arrays

Rob Maaskant
Raj Mittra
Anton Tijhuis

Abstract

A multi-level version of the Characteristic Basis Function Method (CBFM) is presented for computing the input impedance matrix and radiation patterns of very large antenna arrays. Specifically, we consider the challenging problem of an electrically large subarray that is surrounded by (many) other disjoint subarrays, and solve this problem by employing a two-level Characteristic Basis Function Method. At level zero, Rao-Wilton-Glisson (RWG) basis functions are employed to locally synthesize the surface current. Next, the number of degrees of freedom (DoFs) for the current is reduced at level one by employing the characteristic basis functions (CBFs), each of which is a macro basis function supported by an antenna element, and is a fixed combination of RWG basis functions. Moreover, the characteristic basis functions at level two are supported by subarrays to further reduce the degrees of freedom. This multilevel approach is memory efficient and generates a final reduced matrix equation that can be solved directly, i.e., in-core through standard Gaussian elimination techniques, even though the conventional MoM (Method of Moments) formulation of the same problem may require more than one million RWG basis functions. Numerical examples are presented for various array sizes, including a 25 subarray problem comprised of 64 tapered-slot antennas (TSAs) each. The proposed method demonstrates very good accuracy, numerical efficiency, and a reduced memory storage requirement.

1. Introduction

The numerical method presented in this paper has been developed within the framework of the Square Kilometre Array (SKA) project. This is a worldwide endeavor to design and construct a revolutionary new radio telescope with a collecting area which is on the order of one million

square meters, in the wavelength range from 3 m to 1 cm [1-3]. Within this context, the potentials of various array technologies are evaluated by analyzing the impedance as well as the radiation characteristics through electromagnetic-field analyses. In some of these studies, it is vitally important to accurately analyze electrically large – but finite – array antennas and associated truncation effects. Given the electrical size and geometrical complexity of such structures, the numerical analysis presents a severe computational burden, especially when only limited computing resources are available [4, 5].

A wide variety of numerically efficient techniques has been developed over the last few decades to alleviate the above problem. However, in this work we will only consider the class of iteration-free integral-equation techniques, and focus specifically on a recently developed method called the Characteristic Basis Function Method (CBFM). It enhances the conventional Method of Moments by compressing the moment matrix such that the resultant reduced matrix equation can be solved in an iterative-free manner - simultaneously for multiple right-hand sides (MRHS) [6, 7]. The matrix compression is achieved by employing macro basis functions (characteristic basis functions, or CBFs). These are constructed as fixed combinations (aggregations) of subdomain basis functions, each of which is defined over a much smaller support [8, 9]. An even higher compression of the final reduced matrix is achieved through the use of a multilevel version of the Characteristic Basis Function Method. Toward this end, the concept of basis-function aggregation is repeated, such that higher-order characteristic basis functions are expressed in terms of lower-order characteristic basis functions. At the lowest level, the (subdomain) basis functions are chosen to have a simple analytic form, and to conform to arbitrarily shaped geometries, so that the higher-order characteristic basis functions will also satisfy this advantageous geometrical property. An inherent advantage of using these

Rob Maaskant is with the Netherlands Institute for Radio Astronomy (ASTRON), PO Box 2, 7990 AA Dwingeloo, The Netherlands; e-mail: (maaskant@astron.nl). Raj Mittra is with the Electromagnetic Communication Laboratories, Pennsylvania State University, University Park, PA 16802, USA; e-mail: mittra@engr.psu.edu. Anton Tijhuis is with the Faculty of Electrical Engineering, Eindhoven University of Technology, PO Box 513, 5600 MB Eindhoven, The Netherlands; e-mail: a.g.tijhuis@tue.nl.

macro basis functions is that existing computer codes that employ sub-sectional basis functions can be reused with only minor modifications.

Furthermore, in the Characteristic Basis Function Method, the entire computational domain is subdivided into smaller subdomains, each of which supports a set of numerically generated macro basis functions. Such a domain-decomposition technique is advantageous, since many algorithmic steps involved can be carried out in parallel on supercomputers or on platforms with multiple processors [10, 11]. Furthermore, the modular setting of a domain-decomposition technique enables one to analyze/optimize the entire structure at minimal cost by only reconsidering the domains that need to be altered [12].

The concept of reducing the size of the matrix equation by employing numerically generated macro basis functions, and decomposing the problem into smaller problems, has also been widely exploited in other recently developed iterative-free methods for solving large-scale problems. Examples include the Synthetic-Functions Approach (SFX) [13, 14], the Sub-Entire-Domain Basis Function Method (SED) [15], the eigencurrent approach [16], and a subdomain multilevel approach [17]. These methods can be distinguished from each other by the way they generate the macro basis functions, and also by the methods they use to synthesize a junction current between electrically connected subdomains. We note that one can employ a special type of junction basis functions, or an overlapping domain-decomposition technique in which adjacent sets of macro basis functions partially overlap [13, 18].

For electrically large problems, the overall solution time of the Characteristic Basis Function Method is governed by the time it takes to construct the reduced matrix equation, as opposed to solving it. Various acceleration techniques have been proposed to reduce the matrix construction time, including multipole approaches [29, 20]; the Adaptive Cross Approximation (ACA) technique [21]; a multi-level decomposition approach [22]; and the Adaptive Integration Method (AIM) [23]. These methods all rely on the fact that the electric field generated by a macro basis function is a relatively smoothly varying function over the support of the macro test function. This is particularly true if the macro basis and test functions are well separated. Hence, for electrically large antenna and scattering problems, many of the reduced-matrix entries (characteristic basis function reaction integrals) can be rapidly computed.

The reciprocity theorem is often used to compute only the upper-triangular part of the reduced matrix, and this saves approximately a factor of two in the total filling time. More importantly, many reactions between (groups of) characteristic basis functions are replicated elsewhere in the array, because of translation symmetry. Even though the moment matrix may not have a full block-Toeplitz symmetry, many entries (even blocks) of the reduced matrix are thus identical and, hence, can simply be copied during the matrix-construction process.

This paper focuses on the challenging case of large arrays of strongly coupled tapered-slot antennas (TSAs). The radiation and scattering characteristics of such arrays have been considered by others, as well. Much work has been performed on the edge-truncation effects, and the efficient computation of embedded element patterns and element impedances by the authors of [24], both in the time and the frequency domain. In [25], the Finite Element Method was combined with an Integral-Equation technique (FEM-IE) to iteratively solve for the fields in tapered-slot-antenna arrays that involve dielectric materials.

One of the major problems arising in the SKA project is the analysis of large arrays comprising of disjoint phased-array tiles. These structures exhibit multi-scale (quasi-periodic) features, both at the antenna-element level and at the subarray level. To handle these problems, an approximately infinite array approach at the subarray level was developed in [26]. There, the infinite sum was truncated in the spatial domain to compute the scan impedance of antenna elements that were located within an electrically large subarray surrounded by (many) other actively phase-steered subarrays. Basically, the Characteristic Basis Function Method is used here at the antenna-element level, whereas an infinite-array approach is used at the subarray level. Although the method represents a viable alternative to a full-fledged Characteristic Basis Function Method solution, it does not directly yield for us the (passive) input-impedance matrix and embedded element patterns of the antenna array. As a remedy, we propose in this paper to use the Multilevel Characteristic Basis Function Method, since this overcomes the associated memory problems and directly provides us with the impedance and radiation characteristics of all tapered-slot-antenna elements. Note that the capabilities of the Multilevel Characteristic Basis Function Method were already demonstrated for scattering problems in [27].

The paper is organized as follows. First, we provide a brief description of the Multilevel Characteristic Basis Function Method. We describe the steps that are involved in the process of constructing a reduced-matrix equation at all levels, as well as the generation of characteristic basis functions for antenna-type problems. The computation of the input-impedance matrix and radiation patterns are also discussed. Second, the Multilevel Characteristic Basis Function Method is used to compute the radiation patterns and impedances of a 576 tapered-slot-antenna-element array (nine subarrays of 64 tapered-slot antennas each). The results are then compared to those obtained from a mono-level Characteristic Basis Function Method. Third, the problem is enlarged to incorporate 25 subarrays of 64 tapered-slot antennas each. Since the size of this problem exceeds one million RWG basis functions, it renders the problem unmanageable, even when a mono-level Characteristic Basis Function Method approach is used to reduce the size of the associated matrix. However, it will be demonstrated below that the memory requirements can be relaxed when it is solved through a Multilevel Characteristic Basis Function Method approach.

2. Outline of the Multi-Level Characteristic Basis Function Method

2.1 Matrix-Equation Reduction

To understand how the Multilevel Characteristic Basis Function Method achieves its matrix compression, it is instructive to consider the specific example in Figure 1. This depicts an array of two subarrays of two electrically interconnected tapered-slot antennas each. Level-0 in Figure 1 corresponds to the case where the currents are synthesized by M_0 Rao-Wilton-Glisson (RWG) basis functions [28]. The associated matrix equation that needs to be solved reads

$$\mathbf{Z}^{[0]} \mathbf{I}^{[0]} = \mathbf{V}^{[0]}, \quad (1)$$

where the (uncompressed) moment matrix, $\mathbf{Z}^{[0]}$, is of size $M_0 \times M_0$, and where the RWG expansion-coefficient vector is $\mathbf{I}^{[0]} = [I_1^{[0]}, I_2^{[0]}, \dots, I_{M_0}^{[0]}]^T$. The superscript T denotes the

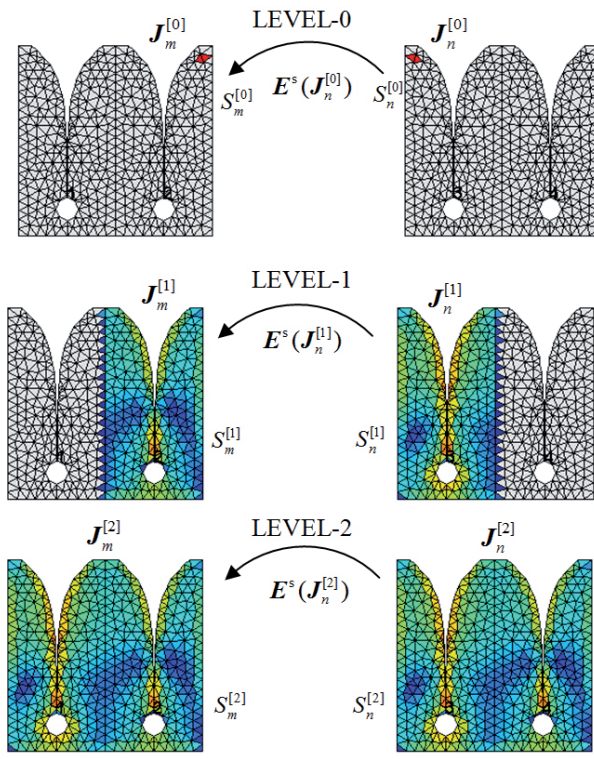


Figure 1. A methodology to compress the moment matrix through a Multilevel Characteristic Basis Function Method approach. Level-1: reactions between RWG basis functions. Level-2: reactions between characteristic basis functions supported by antenna elements (plus a single-cell extension). Level-3: reactions between characteristic basis functions supported by subarrays

transpose, and $\mathbf{V}^{[0]}$ is the excitation vector. In the following, we will assume that the matrix equation is very large and cannot be solved through standard Gaussian-elimination techniques.

For perfectly conducting sheets, and when Galerkin's scheme is used for testing the electric-field integral equation through a symmetric product, the moment matrix in Equation (1) is symmetric and the elements are recognized as reaction integrals. The matrix element $Z_{mn}^{[0]}$ thus denotes the radiated electric field, \mathbf{E}^s , generated by the n th RWG basis function $\mathbf{J}_n^{[0]}$, which is tested over the support, $S_m^{[0]}$ of basis function $\mathbf{J}_m^{[0]}$ (see also Figure 1). The matrix element can be written as

$$Z_{mn}^{[0]} = \int_{S_m^{[0]}} \mathbf{J}_m^{[0]} \cdot \mathbf{E}^s (\mathbf{J}_n^{[0]}) dS, \quad (2)$$

with $m, n \in \{1, 2, \dots, M_0\}$. Furthermore, the m th element of the excitation vector $\mathbf{V}^{[0]}$ is expressed in terms of the incident electric field \mathbf{E}^{inc} as

$$V_m^{[0]} = - \int_{S_m^{[0]}} \mathbf{J}_m^{[0]} \cdot \mathbf{E}^{inc} dS. \quad (3)$$

It is pointed out that the matrix Equation (1) is significantly smaller when we employ a set of M_1 macro-domain basis functions, $\{\mathbf{J}_m^{[1]}\}_{m=1}^{M_1}$, with $M_1 \ll M_0$. One then needs to solve the relatively small-size matrix equation $\mathbf{Z}^{[1]} \mathbf{I}^{[1]} = \mathbf{V}^{[1]}$, where the matrix $\mathbf{Z}^{[1]}$ is of size $M_1 \times M_1$. The elements of $\mathbf{Z}^{[1]}$ and $\mathbf{V}^{[1]}$ are defined through Equations (2) and (3), respectively, where the 0 index is replaced by 1. In the Characteristic Basis Function Method, the macro basis functions are called characteristic basis functions (CBFs), and are expressed in terms of a fixed combination of lower-level basis functions. For instance, at level-1 (see Figure 1), the m th characteristic basis function $\mathbf{J}_m^{[1]}$ is expressed in terms of the M_0 RWG basis functions $\{\mathbf{J}_m^{[0]}\}$ at level-0 as

$$\mathbf{J}_m^{[1]} = \sum_{m=1}^{M_0} I_m^{CBF;[0]} \mathbf{J}_m^{[0]}, \quad (4)$$

where the $I_m^{CBF;[0]}$ are predetermined RWG expansion coefficients describing the “shape” of the m th characteristic basis function $\mathbf{J}_m^{[1]}$. Note that for antenna problems, it is natural to take the support of the level-1 characteristic basis functions to be equal to the size of a single antenna element (as in Figure 1), particularly because the degree of translation symmetry for array antennas is largest at the antenna-element level. Hence, the characteristic basis functions have a local support, and many RWG expansion coefficients in Equation (4) will be zero. The determination of the expansion

coefficients in Equation (4) will be described in Section 2.3, where we also explain the single-cell extension in the overlapping region, as shown in Figure 1.

Once the level-1 characteristic basis functions have been generated, the elements of the reduced matrix $\mathbf{Z}^{[1]}$ can be computed. For instance, and with reference to Equation (2), the matrix element $Z_{mn}^{[1]}$ (with $m, n \in \{1, 2, \dots, M_1\}$) is computed as

$$\begin{aligned} Z_{mn}^{[1]} &= \int_{S_m^{[1]}} \mathbf{J}_m^{[1]} \cdot \mathbf{E}^s \left(\mathbf{J}_n^{[1]} \right) dS \\ &= \sum_{m=1}^{M_0} \sum_{n=1}^{M_0} I_m^{\text{CBF};[0]} \left[\int_{S_m^{[0]}} \mathbf{J}_m^{[0]} \cdot \mathbf{E}^s \left(\mathbf{J}_n^{[0]} \right) dS \right] I_n^{\text{CBF};[0]} \quad (5) \\ &= \left(\mathbf{I}^{\text{CBF}m;[0]} \right)^T \mathbf{Z}^{[0]} \mathbf{I}^{\text{CBFn};[0]}, \end{aligned}$$

where we have made use of Equation (4) and the linearity of the operators in computing the scattered field, \mathbf{E}^s . The column vector $\mathbf{I}^{\text{CBFn};[0]}$ holds the RWG expansion coefficients of the n th characteristic basis function $\mathbf{J}_n^{[1]}$ at level-1. Because the vectors $\mathbf{I}^{\text{CBF}m;[0]}$ and $\mathbf{I}^{\text{CBFn};[0]}$ contain many zero entries, effectively, only the matrix block $\mathbf{Z}_{mn}^{[0]}$ of $\mathbf{Z}^{[0]}$ in Equation (5) is required, namely the matrix that corresponds to the RWG basis functions on the observation and the source domains $S_m^{[1]}$ and $S_n^{[1]}$ (see Figure 1, level-1), respectively. In the following, we will therefore discard the zeros in the expansion-coefficient vectors, and instead work with the much-smaller matrix block $\mathbf{Z}_{mn}^{[0]}$, and the expansion-coefficient vectors $\mathbf{I}_m^{\text{CBF};[0]}$ and $\mathbf{I}_n^{\text{CBF};[0]}$ that are associated with the local supports $S_m^{[1]}$ and $S_n^{[1]}$, respectively.

Following the above methodology, we move to the next higher level (level-2) and increase the support of the characteristic basis functions, as shown in Figure 1, where a characteristic basis function occupies an entire subarray. From Equation (5), it is then evident that an element of the reduced matrix $\mathbf{Z}^{[2]}$ can be expressed in terms of the elements of $\mathbf{Z}^{[1]}$ in conjunction with the characteristic-basis-function expansion coefficients at level-1.

In general, at the i th level ($i = 1, 2, \dots$), one observes that

$$Z_{mn}^{[i]} = \left(\mathbf{I}_m^{\text{CBF};[i-1]} \right)^T \mathbf{Z}_{mn}^{[i-1]} \mathbf{I}_n^{\text{CBF};[i-1]}. \quad (6)$$

For an element $V_m^{[i]}$ of the excitation vector $\mathbf{V}^{[i]}$,

$$V_m^{[i]} = \left(\mathbf{I}_m^{\text{CBF};[i-1]} \right)^T \mathbf{V}_m^{[i-1]}, \quad (7)$$

where one observes that Equations (6) and (7) are both written in terms of a recursive formula [27].

It is assumed that the matrix equation at the highest level can be solved directly, after which the expansion coefficients for the current can be computed at any lower level through the recursive version of Equation (4).

According to the above-described Multilevel Characteristic Basis Function Method, the general procedure for solving the large matrix Equation (1) consists of the following steps:

1. Generate characteristic basis functions at level-1 by extracting small subarrays from the fully meshed antenna array (equipped with RWG basis functions), and subsequently excite them to generate primary and secondary characteristic basis functions (see Section 2.3). If the final radiation pattern is of interest, then also compute the far-field patterns of the characteristic basis functions at level-1. Superimpose these to form the total radiation pattern, once the characteristic-basis-function expansion coefficients at level-1 are known (see Step 3).
2. Rapidly construct $\mathbf{Z}^{[1]}$ through the Adaptive Cross Approximation (ACA) algorithm, as was described in [21]. In addition, exploit reciprocity and take advantage of the fact that many rank-deficient block matrices associated with group pairs of characteristic basis functions at level-1 are identical, and, hence, can be simply copied during the construction of the matrix $\mathbf{Z}^{[1]}$ [26].
3. Generate characteristic basis functions at level-2 by extracting larger subarrays from the fully meshed antenna array, and subsequently excite them to generate primary and secondary characteristic basis functions at level-2. To be able to solve for the excitations of each of these larger subarray problems, we make use of the Characteristic Basis Function Method at the lower level, i.e., level-1. The level-2 characteristic basis functions are thus expressed in terms of the level-1 characteristic basis functions by using their expansion coefficients (see Equation (4)). These coefficients are also used to determine the level-2 characteristic-basis-function far-field patterns, because each of these is a superposition of level-1 characteristic-basis-function patterns (see Section 2.2).
4. Continue by generating characteristic basis functions at level i with the aid of the Characteristic Basis Function Method approach at the level $i-1$ (for $i = 3, 4, \dots$), and compute a new set of characteristic-basis-function patterns.

5. Construct and solve the reduced matrix equation for the full problem only at the highest level for a certain (reduced) set of excitation vectors. Afterwards, the antenna input-impedance matrix is computed from the expansion-coefficient vector and the reduced matrix at the highest level (*cf.* Section 2.2). The total radiation pattern is computed directly with the aid of this characteristic-basis-function expansion-coefficient vector and the last-determined set of characteristic-basis-function patterns. If required – for example, to visualize the surface-current distribution – the solution at the lowest level (for the RWG basis) can be recovered through the recursive version of Equation (4).

2.2 Computation of the Far-Field Pattern and Input Impedance Matrix through the Multilevel Characteristic Basis Function Method

The m th characteristic-basis-function far-field function $\mathbf{f}_m^{\text{CBF};[i]}$ at the level i can be expanded in terms of the M_{i-1} characteristic-basis-function far-field patterns $\{\mathbf{f}_m^{\text{CBF};[i-1]}\}$ at the lower level $i-1$ as follows:

$$\mathbf{f}_m^{\text{CBF};[i]}(\theta, \phi) = \sum_{m=1}^{M_{i-1}} I_m^{\text{CBF};[i-1]} \mathbf{f}_m^{\text{CBF};[i-1]}(\theta, \phi), \quad (8)$$

where $I_m^{\text{CBF};[i-1]}$ is the m th expansion coefficient for the m th characteristic basis function at the level $i-1$. The coefficient vector $\mathbf{I}^{\text{CBF};[i-1]}$ is computed via the Characteristic Basis Function Method for a certain array excitation. In the process of computing the characteristic-basis-function patterns at each level, one should realize that many of the subdomains support the same set of characteristic basis functions, so that the respective characteristic-basis-function patterns are identical as well, apart from a phase correction due to their translated position. For instance, we can write

$$\mathbf{f}_p^{\text{CBF};[i]} = \mathbf{f}_q^{\text{CBF};[i]} \exp[-jk \mathbf{r}_{pq} \cdot \hat{\mathbf{r}}(\theta, \phi)], \quad (9)$$

where the p th characteristic-basis-function pattern at the level i is derived from the q th pattern by accounting for the translation vector, \mathbf{r}_{pq} . The unit vector $\hat{\mathbf{r}}(\theta, \phi)$ denotes the direction of observation, and k is the free-space wavenumber of the medium. Finally, it is obvious that the total array far-field pattern, $\mathbf{f}^{[i]}$, which is the quantity of interest at the highest level, can also be expanded in terms of the characteristic basis functions and associated expansion coefficients at the lower level $i-1$.

In the solution of the electric-field integral equation, it is straightforward to use voltage generators and to short circuit the other terminals, so that the antenna input-admittance matrix is obtained naturally. The mutual admittance, Y_{ab}^{ant} , between two accessible ports a and b , can be computed in terms of a reaction integral, which is of a variational form. Suppose that \mathbf{J}_a is the array surface-current distribution that results from exciting terminal a with a voltage source of amplitude V_a , while all other terminals are short-circuited. Likewise, \mathbf{J}_b is a result of exciting terminal b with V_b , while all other terminals are short-circuited. A stationary formula for the mutual antenna admittance, Y_{ab}^{ant} , was been in [29] with the aid of the Lorentz reciprocity theorem. The resulting expression is

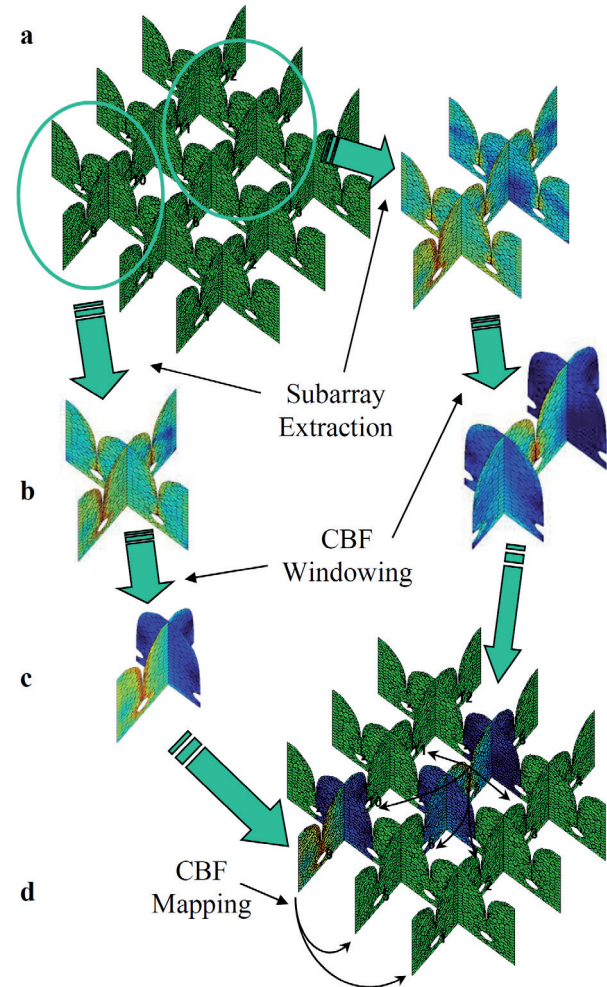


Figure 2. An approach to generate and window primary characteristic basis functions for the transmitting case: (i) Subarray extraction and generation of primary characteristic basis functions; (ii) Trapezoidal post-windowing of characteristic basis functions; (iii) One-to-one mapping of characteristic basis functions throughout the array lattice.

$$Y_{ab}^{\text{ant}} = -\frac{1}{V_a V_b} \int_{S_a} \mathbf{J}_a \cdot \mathbf{E}^s(\mathbf{J}_b) dS \quad (10)$$

$$= -\frac{1}{V_a V_b} \left(\mathbf{I}_a^{CBF;[i-1]} \right)^T \mathbf{Z}^{[i-1]} \mathbf{I}_b^{CBF;[i-1]},$$

where the solutions at the level i for the currents \mathbf{J}_a and \mathbf{J}_b have been substituted in terms of the characteristic-basis-function expansion-coefficient vectors at the lower level $i-1$ (*cf.* Equation (5)). It is important to note that a minus sign appears in front of Equation (10), which is contrary to the plus sign presented earlier in [21] and in [30, p. 109].

2.3 Generation and Windowing of Characteristic Basis Functions at all Levels

A rather attractive feature of the Characteristic Basis Function Method is the way the physics-based characteristic basis functions are generated. We will briefly describe this procedure at level-1 for an overlapping domain-decomposition approach, applied to antenna-array problems for transmitting. The details can be found in several previously published works [18, 21] and [26].

For large antenna-array problems, we first extract several distinct and relatively small subarrays from the fully meshed array, typically from the center, corners, and edges of the array. The subarray sizes are chosen such that the direct electromagnetic environment for the center, corner, and edge elements of the corresponding subarrays closely resemble their original electromagnetic-array environment. For instance, Figure 2b illustrates two subarrays that are extracted from a $4 \times 3 \times 2$ dual-polarized Vivaldi array (four elements in the E plane, three elements in the H plane, and two polarizations). These two subarrays represent a corner and center element, along with their interconnected neighboring elements, respectively.

Next, we solve for a set of surface currents induced in each of the subarrays by sequentially exciting the antenna terminals of the corresponding subarray (Figure 1b). Hence, for this example, four primary characteristic basis functions are generated for the subarray comprising the corner element, and seven primary characteristic basis functions are generated for the subarray comprising the center element.

We next apply a (trapezoidal) post-windowing function to the sets of primary characteristic basis functions (in Figure 1b) to suppress the undesired edge-truncation effects by reducing the support of the so-generated primary characteristic basis functions (Figure 1c). In essence, the

RWG expansion coefficients making up the characteristic basis functions are post-multiplied with suitable weights. Note that the partially overlapping windowing functions have to add up to unity, so that the tapered characteristic basis functions add up in a correct manner as well, particularly in the overlapping regions.

In our specific example (Figure 1), the support covers half of the neighboring elements, although this can be changed in a manner discussed in [18]. For instance, in [21], very good accuracy was realized with only a single-cell overlap.

Finally, the set of characteristic basis functions are mapped, one-to-one, onto the corresponding edge and center elements, so that each array-element/subdomain will have its own set of characteristic basis functions (Figure 1d). Note that for this example, six subarrays have to be extracted in total to accommodate characteristic basis functions on all the array elements (three subarrays per polarization, i.e., two subarrays for the opposite-edge elements, and one for a center element).

The number of characteristic basis functions on array elements can be enlarged in order to model surface currents on array elements that can have a large number of degrees of freedom. This can be done by appending a set of secondarily generated characteristic basis functions to the already existing set of primary characteristic basis functions [7]. This is accomplished by taking the primary characteristic basis functions as distant current sources irradiating the subarrays. The thus generated currents then induce extra surface currents on these subarrays, after which these newly generated currents are truncated/windowed again, and added to the primary set of characteristic basis functions. Finally, one needs to ortho-normalize the characteristic basis functions, and retain only a minimal number of them. Both of these steps can be accomplished with the aid of a singular-value decomposition (SVD), and a thresholding procedure on the singular values [31, 32].

The above procedure is repeated to generate the characteristic basis functions for the higher levels. The only difference is that we will have to employ a lower-level Characteristic Basis Function Method to be able to solve for the subarray currents.

A rigorous full-wave analysis of phased-array antennas, each of which is surrounded by a number of other disjoint antenna arrays, becomes computationally prohibitive whenever we consider a large number of electrically large subarrays. A mono-level Characteristic Basis Function Method employs a relatively small number of characteristic basis functions, thereby reducing the computational complexity of solving the matrix equation by a large factor. However, beyond a certain point, the numerical analysis of a much-larger array of subarrays will inevitably pose a computational burden, which is caused by an increase in the number of unknowns.

To alleviate the associated memory problems, we propose to use the two-level Characteristic Basis Function Method, as outlined in Figure 1. This first generates characteristic basis functions at the antenna-element level, after which the characteristic basis functions are generated for each of the subarrays. The accuracy and computational efficiency is demonstrated below for various antenna array sizes.

All the computations were carried out by using double-precision arithmetic on a Dell Inspiron 9300 notebook, equipped with an Intel Pentium-M processor operating at 1.73 GHz, and 2.0 GB of RAM.

The tapered-slot antenna-element geometry was adopted from [18] and [21], and serves here as a reference case for further study.

2.4 An Array of Two Subarrays of Two Tapered-Slot Antenna Elements Each

We will first examine the accuracy of the Multilevel Characteristic Basis Function Method for a relatively small antenna-array problem, so that the direct MoM solution can be used as a reference for the purpose of validation. Specifically, the antenna subarray problem in Figure 1 is solved, for which we disable the Adaptive Cross Approximation algorithm, and set the singular-value-decomposition threshold in the Characteristic Basis Function Method to zero. This implies that we will employ all the primary and secondary characteristic basis functions that have been generated. The radius for generating the secondary basis functions is set large enough so as to include all the neighboring antenna-array elements at level-1, and all the neighboring subarrays at level-2. The relative error in the computed antenna input-impedance matrix is defined as

$$Error\% = \frac{\|\mathbf{Z}_{MoM}^{ant} - \mathbf{Z}_{CBFM}^{ant}\|_F}{\|\mathbf{Z}_{MoM}^{ant}\|_F} \times 100\%, \quad (11)$$

where $\|\cdot\|_F$ denotes the Frobenius norm, which takes the square root of the sum of the absolute squares of the matrix elements.

Quantity	Level-0 (Direct MoM)	Level-1 CBFM	Level-2 MLCBFM
#RWGs	2534	2534	2534
#CBFs (Level-1)	—	40	40
#CBFs (Level-2)	—	—	12
Generation time CBFs	0 min 0 sec	2 min 28 sec	2 min 41 sec
Total execution time	1 min 20 sec	5 min 48 sec	5 min 57 sec
Relative error \mathbf{Z}^{ant}	0%	0.0267%	0.0266%

Table 1 illustrates that the number of basis functions was reduced from 2534 RWG basis functions for a direct MoM to only 12 characteristic basis functions (the matrix compression was 99.998%) for a level-2 Characteristic Basis Function Method. Furthermore, the relative error of a level-2 Characteristic Basis Function Method is much smaller than one percent and is—remarkably enough for this specific example—almost equal to the accuracy of a level-1 Characteristic Basis Function Method. Not unexpectedly, the total execution time was smallest for a direct MoM approach, particularly because the Characteristic Basis Function Method requires an additional amount of time to generate the characteristic basis functions and to construct a reduced matrix equation. On the contrary, in a classical MoM approach, the total execution time is governed by the time to solve the matrix equation, as it scales with the cube of the number of independent basis functions: consequently, it is advantageous to reduce the number of independent basis functions. Once this reduction has been achieved—for instance, through the use of the Multilevel Characteristic Basis Function Method—then the upper limit of the solution time is determined by the largest matrix equation that can still be solved in-core (typically, the matrix size must remain smaller than 7000×7000).

Figures 3 and 4 illustrate the E- and H-plane cuts of the computed embedded element patterns (150 ohm port termination) in the case where element 1 and, subsequently, element 2 was excited. One observes that the numerical results, as computed by a direct MoM approach, a level-1 Characteristic Basis Function Method, and a level-2 Characteristic Basis Function Method, were visually indistinguishable from each other. This was also confirmed by the low relative error in the numerically computed input-impedance matrix of the antenna (see Table 1).

2.5 Nine Subarrays Composed of 64 Tapered-Slot-Antenna Elements Each

The numerical accuracy and efficiency of a two-level Characteristic Basis Function Method approach, relative to a mono-level Characteristic Basis Function Method approach, will be evaluated in this section, for an array of nine disjoint subarrays of 64 tapered-slot-antenna elements each.

Table 1. A comparison between a direct MoM approach, a mono-level, and a level-2 Multilevel Characteristic Basis Function Method in reducing the number of independent basis functions, the generation time of basis functions, and the total solution time (at 900 MHz).

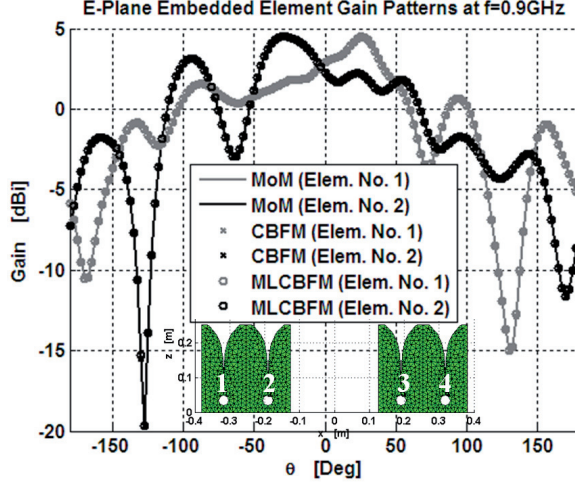


Figure 3. The computed E-plane element-gain patterns at 900 MHz. The results were computed through a direct MoM approach, a 1-level Characteristic Basis Function Method, and a 2-level Characteristic Basis Function Method.

The anomalous antenna-impedance effects, associated with the (resonant) gaps/slots between disjoint subarray tiles, were reported in [33, 34], and will therefore not be discussed in this paper. These gaps may need to be introduced for servicing purposes, so that, e.g., individual subarrays can be installed and/or removed as modular units. Furthermore, the transport and manufacturability of relatively small units may be advantageous.

The numerical computations were performed for a singular-value-decomposition threshold level of 10^{-2} (used to reduce and retain a minimal set of basis function at each level of the Multilevel Characteristic Basis Function Method). The Adaptive Cross Approximation threshold, which was used to rapidly construct the low-rank (off-diagonal) moment-matrix blocks, was set to 10^{-3} . Numerical experiments showed that a reduced Adaptive Cross Approximation threshold level has a positive effect on the symmetry of the input-impedance matrix. Furthermore, it suppresses the spurious ripples that the

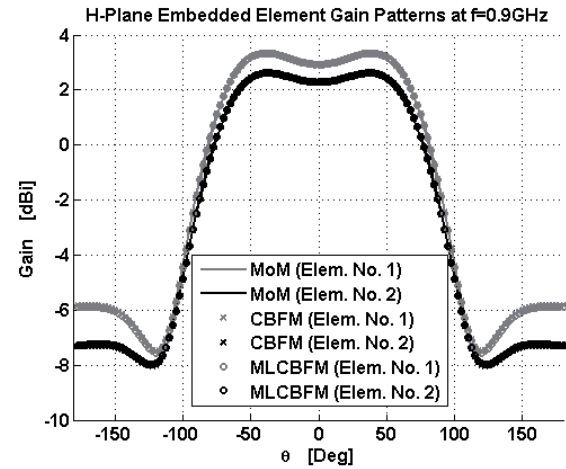


Figure 4. The computed H-plane element-gain patterns at 900 MHz. The results were computed through a direct MoM approach, a 1-level Characteristic Basis Function Method, and a 2-level Characteristic Basis Function Method.

element radiation patterns may exhibit, albeit at a cost of longer matrix filling time. At level-1, the radius for generating the secondary characteristic basis functions was taken equal to the width of two antenna elements, whereas it was enlarged at level-2 to incorporate all the surrounding subarrays. We also studied the case in which we bypassed the generation of secondary characteristic basis functions at level-2.

Figures 6a and 6b illustrate the E-plane cuts of the power beam pattern of two subarrays, i.e., of the central and edge tiles on the right-hand side of the central tile (secondary characteristic basis functions included). The tiles were subsequently scanned to broadside ($\theta_{\text{scan}} = 0^\circ$), and to an off-broadside direction ($\theta_{\text{scan}} = 60^\circ$). The level-1 and level-2 Characteristic Basis Function Method were found to yield very similar results. The agreement slightly degraded when the beam was scanned to off-broadside directions. This was expected, because the (active) mutual coupling between the tiles increased for off-broadside scan

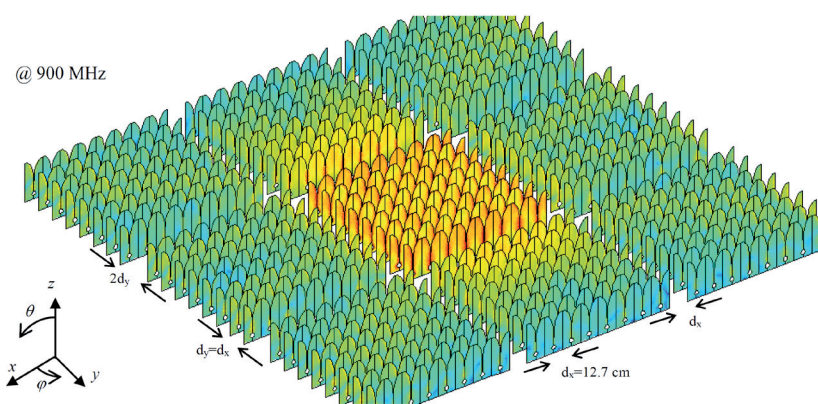


Figure 5. An array of nine subarrays (3×3) (see also [26]), each of them composed of 64 tapered-slot-antenna elements (8×8). To illustrate coupling effects, the active antennas within the central tile were excited by a voltage-gap generator placed across the slot of each tapered-slot-antenna element. The central tile scanned to broadside (end-fire direction), whereas the tapered-slot antennas of the surrounding tiles were short-circuited. The magnitude of the surface-current distribution is shown (log scale) as computed by a direct Characteristic Basis Function Method approach.

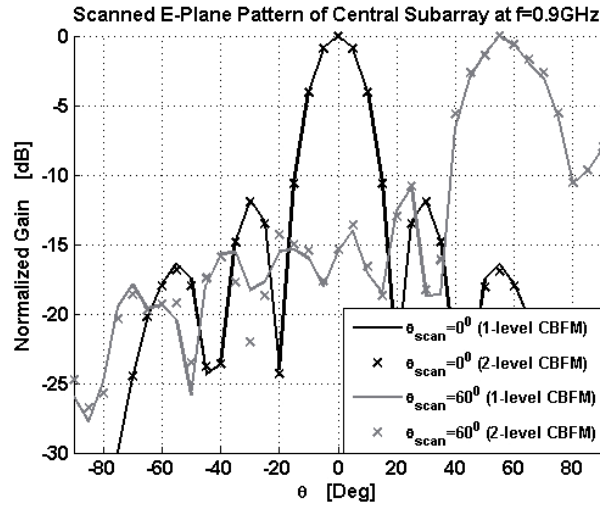


Figure 6a. E-plane cuts of the power pattern (at 900 MHz) of a subarray beam for the central tile when scanned to broadside ($\theta_{\text{scan}} = 0^\circ$), and to an off-broadside direction ($\theta_{\text{scan}} = 60^\circ$), for both a level-1 and level-2 Characteristic Basis Function Method.

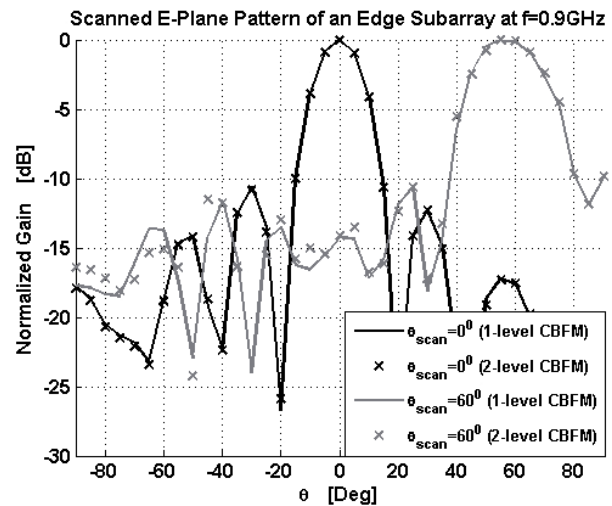


Figure 6b. E-plane cuts of the power pattern (at 900 MHz) of a subarray beam for an edge tile (to the right of the center tile: see Figure 5) when scanned to broadside ($\theta_{\text{scan}} = 0^\circ$), and to an off-broadside direction ($\theta_{\text{scan}} = 60^\circ$), for both a level-1 and level-2 Characteristic Basis Function Method.

directions. In these cases, the antenna tile that was excited also illuminated the neighboring tiles, so that a more-accurate numerical scheme was required than for a broadside-scanned beam.

Not surprisingly, the relative error of the numerically computed antenna input-impedance matrix in Table 2 reduced from 15.6% to 4.5% when the secondary characteristic basis functions at level-2 were included. This error reduction required almost twice the amount of characteristic basis functions, but did not lead to a much longer simulation time, because the construction of the reduced matrix was the most time-demanding element in the process.

The reduction in the number of unknowns was seen to be rather significant. The original problem (level-0) required 375,192 RWG basis functions, which was reduced to only 4320 by a level-1 Characteristic Basis Function Method approach. The degrees of freedom for the current was reduced even further at level-2, down to 1116. Since the total execution time increased only slightly, it supported the conclusion of [27], namely that the Multilevel Characteristic Basis Function Method is a memory-efficient implementation of a mono-level Characteristic Basis Function Method.

Quantity	Level-1 CBFM	Level-2 CBFM (Primary CBFs at Level-2 Only)	Level-2 CBFM (Primary + Secondary CBFs)
#RWGs	375192	375192	375192
Time to generate the mesh	32 min 11 sec	1 min 38 sec	1 min 38 sec
#MoM blocks to be constructed, exploiting reciprocity and translation symmetry	4770 out of 331776	4770 out of 331776	4770 out of 331776
#Primary CBFs (Level-1)	1584	1584	1584
#Primary + secondary CBFs (Level-1)	4320	4320	4320
#Primary CBFs (Level-2)	–	576	576
#Primary + secondary CBFs (Level-2)	–	576 (one CBF per antenna element)	1116
Generation time CBFs	9 min 11 sec	17 min 39 sec	23 min 58 sec
Total execution time (excludes meshing time)	151 min 46 sec	160 min 14 sec	166 min 33 sec
Relative error Z^{ant}	0%	15.6%	4.5%

Table 2. The required computational resources and execution time for a level-1 and for two level-2 Characteristic Basis Function Method approaches (at 900 MHz).

# RWGs (level-0)	# CBFs (level-1)	# CBFs (level-2)	# MoM blocks	# MoM blocks (Exploiting Symmetry and Reciprocity)	Time to Build MoM Blocks	Total Execution Time
1042200	12000	3100	2560000	14574	323 min 55 sec	667 min 33 sec

Table 3. The required computational resources and execution time for a level-2 CBFM approach (at 900 MHz, with 25 antenna tiles).

2.6 25 Subarrays Composed of 64 Tapered-Slot-Antenna Elements Each

Next, we present the results for a very large antenna array, one that could no longer be solved by using the mono-level Characteristic Basis Function Method. We considered an antenna array consisting of 25 subarrays, each comprised of 64 tapered-slot-antenna elements (see Figure 7). The problem required more than one million RWG basis functions (at level-0), and the number of level-1 characteristic basis functions exceeded 10,000 (see Table 3). The problem was solved in-core through standard Gaussian-elimination techniques at level-2, where the number of characteristic basis functions was as low as 3100. For this simulation, we used the Characteristic Basis Function Method-Adaptive Cross Approximation settings as mentioned in the previous section. The total execution time was just over 11 hours, most of which was devoted to filling the blocks of the moment matrix. The approximate time for assembling the reduced matrix was ~176 min; for computing the reduced set of excitation vectors, ~103 min;

for solving the reduced matrix at level-2 (3100×3100) and computing the antenna impedance matrix, ~22 min; and the remaining time was spent on the generation of the primary and secondary characteristic basis functions. It is worth pointing out that the mesh generation took only 18 min 9 sec, because advantage was taken of the fact that a large degree of translation symmetry existed at all levels for regularly-spaced antenna arrays.

3. Conclusions

In this paper, we have presented a multi-level version of the numerically efficient Characteristic Basis Function Method (CBFM) for computing the input-impedance matrix and radiation patterns of very large antenna arrays. Numerical examples have been presented for various array sizes, including a 25 subarray problem of 64 tapered-slot antennas (TSAs) each, which required more than one million RWG basis functions. The proposed method demonstrated very good accuracy, numerical efficiency, and a reduced memory-storage requirement. This led us to conclude that the Multilevel Characteristic Basis Function Method algorithm is memory efficient, and it generates a final reduced matrix equation that can be solved directly, in-core, using standard Gaussian-elimination techniques. Hence, the Multilevel Characteristic Basis Function Method extends the capabilities of the mono-level Characteristic Basis Function Method, and is useful for solving large antenna (and scattering) problems. Finally, we note that the total execution time in the Multilevel Characteristic Basis Function Method is only slightly higher, primarily because of the overhead related to the generation of characteristic basis functions.

4. Acknowledgment

This work was sponsored by the Square Kilometre Array (SKA) Aperture Array Verification Program (AAVP), and the Netherlands Organization for Scientific Research (NWO).

5. References

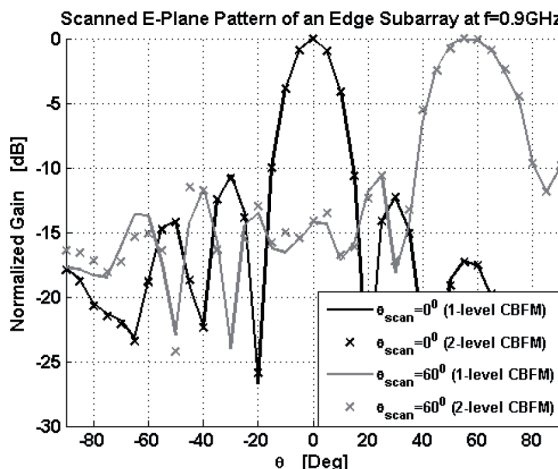


Figure 7. An array of 25 subarrays (5×5), each of them composed of 64 tapered-slot-antenna elements (8×8). To illustrate coupling effects, the active antennas within the central tile were excited by a voltage-gap generator placed over the slot of each tapered-slot-antenna element. The central tile scanned to broadside (end-fire direction), whereas the tapered-slot antennas of the surrounding tiles were short-circuited. The magnitude of the surface-current distribution is shown on a log scale (80 dB dynamic range).

- P. J. Hall, "The Square Kilometre Array: An Engineering Perspective," (reprinted from *Experimental Astronomy*, **17**, 1-3, 2004), Berlin, Springer, 2005, ISBN: 1-4020-3797-x.

2. A. B. Smolders and M. P. van Haarlem, "Perspectives on Radio Astronomy: Technologies for Large Antenna Arrays," Conference Proceedings ASTRON, April 1999, , ISBN: 90-805434-2-x.
3. <http://www.skatelescope.org/>.
4. R. Mittra, "A Look at Some Challenging Problems in Computational Electromagnetics," *IEEE Antennas and Propagation Magazine*, **46**, 5, October 2004, pp. 18-32.
5. R. Maaskant, M. Ivashina, R. Mittra, W. Yu, and N.-T. Huang, "Parallel FDTD Modeling of a Focal Plane Array with Vivaldi Elements on the Highly Parallel LOFAR Bluegene/L Supercomputer," IEEE International Symposium on Antennas and Propagation Digest, Albuquerque, New Mexico, July 2006, pp. 3861-3864.
6. V. Prakash and R. Mittra, "Characteristic Basis Function Method: A New Technique for Efficient Solution of Method of Moments Matrix Equations," *Micr. Opt. Technol.*, **36**, January 2003, pp. 95-100.
7. J. Yeo, V. Prakash, and R. Mittra, "Efficient Analysis of a Class of Microstrip Antennas Using the Characteristic Basis Function Method (CBFM)," *Micr. Opt. Technol.*, **39**, December 2003, pp. 456-464.
8. G. A. E. Vandenbosch and A. R. Van de Cappelle, "Use of Combined Expansion Scheme to Analyze Microstrip Antennas with the Method of Moments," *Radio Science*, **27**, November/December 1992, pp. 911-916.
9. J. Heinstadt, "New Approximation Technique for Current Distribution in Microstrip Array Antennas," *Micr. Opt. Technol.*, **29**, October 1993, pp. 1809-1810.
10. E. Lucente and A. Monorchio, "A Parallel Iteration-Free MoM Algorithm Based on the Characteristic Basis Function Method," International URSI Commission B EM Theory Symposium, EMTS 2007, July 26-28, 2007, Ottawa, Canada.
11. D. J. Ludick and D. B. Davidson, "Investigating Efficient Parallelization Techniques for the Characteristic Basis Function Method (CBFM)," Proceedings of the International Conference on Electromagnetics in Advanced Application (ICEAA), Torino, September 2009, pp. 400-403.
12. A. M. van de Water, B. P. de Hon, M. C. van Beurden, A. G. Tijhuis, and P. de Maagt, "Linear Embedding via Green's Operators: A Modeling Technique for Finite Electromagnetic Band-Gap Structures," *Phys. Rev. E*, **72**, 2005, 056704.
13. L. Matekovits, V. A. Laza, and G. Vecchi, "Analysis of Large Complex Structures with the Synthetic-Functions Approach," *IEEE Transactions on Antennas and Propagation*, **AP-55**, 9, September 2007, pp. 2509-2521.
14. L. Matekovits, G. Vecchi, G. Dassano, and M. Orefice, "Synthetic Function Analysis of Large Printed Structures: The Solution Space Sampling Approach," IEEE International Symposium on Antennas and Propagation, Boston, Massachusetts, July 2001, pp. 568-571.
15. W. B. Lu, T. J. Cui, Z. G. Qian, X. X. Yin, and W. Hong, "Accurate Analysis of Large-Scale Periodic Structures Using an Efficient Sub-Entire-Domain Basis Function Method," *IEEE Transactions on Antennas and Propagation*, **AP-52**, 11, November 2004, pp. 3078-3085.
16. D. J. Bekers, S. J. L. van Eijndhoven, A. A. F. van de Ven, P. Borsboom, and A. G. Tijhuis, "Eigencurrent Analysis of Resonant Behavior in Finite Antenna Arrays," *IEEE Transactions on Microwave Theory and Techniques*, **54**, 6, June 2006, pp. 2821-2829.
17. E. Suter, J. R. Mosig, "A Subdomain Multilevel Approach for the Efficient MoM Analysis of Large Planar Antennas," *Micr. Opt. Technol.*, **26**, 4, August 2000, pp. 270-277.
18. R. Maaskant, R. Mittra, and A. G. Tijhuis, "Application of Trapezoidal-Shaped Characteristic Basis Functions to Arrays of Electrically Interconnected Antenna Elements," Proceedings of the International Conference on Electromagnetics in Advanced Application (ICEAA) 2007, September 17-21, 2007, pp. 567-571.
19. C. Craeye, "A Fast Impedance and Pattern Computation Scheme for Finite Antenna Arrays," *IEEE Transactions on Antennas and Propagation*, **AP-54**, 10, October 2006, pp. 3030-3034.
20. E. Garcia, C. Delgado, F. S. de Adana, F. Cátedra, and R. Mittra, "Incorporating the Multilevel Fast Multipole Method into the Characteristic Basis Function Method to Solve Large Scattering and Radiation Problems," IEEE International Symposium on Antennas and Propagation, Honolulu, Hawaii, June 2007, pp. 1285-1288.
21. R. Maaskant, R. Mittra, and A. G. Tijhuis, "Fast Analysis of Large Antenna Arrays Using the Characteristic Basis Function Method and the Adaptive Cross Approximation Algorithm," *IEEE Transactions on Antennas and Propagation*, **AP-56**, 11, pp. 3440-3451, November 2008.
22. I. Stevanovic, and J. R. Mosig, "Subdomain Multilevel Approach with Fast MBF Interactions," IEEE International Symposium on Antennas and Propagation, Monterey, California, June 2004, pp. 367-370.
23. P. De Vita, A. Freni, L. Matekovits, P. Pirinoli, and G. Vecchi, "A Combined AIM-SFX Approach for Large Complex Arrays," IEEE International Symposium on Antennas and Propagation, Honolulu, Hawaii, June 2007, pp. 3452-3455.
24. C. Craeye, A. O. Boryssenko, and D. H. Schaubert, "Analysis of Infinite and Finite Arrays of Tapered-Slot Antennas for SKA," Proc. EUMC, Milan, Italy, 2002, pp. 1003-1006.
25. M. N. Vouvakis, S.-C. Lee, K. Zhao, and J.-F. Lee, "A Symmetric FEM-IE Formulation with a Single-Level IE-QRA Algorithm for Solving Electromagnetic Radiation and Scattering Problems," *IEEE Transactions on Antennas and Propagation*, **AP-52**, 11, November 2004, pp. 3060-3070.
26. R. Maaskant, R. Mittra, and A. G. Tijhuis, "Fast Solution of Multi-Scale Antenna Problems for the Square Kilometre Array (SKA) Radio Telescope Using the Characteristic Basis Function Method (CBFM)," *Applied Computational Electromagnetics Society (ACES) Journal*, **24**, 2, April 2009, pp. 174-188.

27. J. Laviada, F. Las-Heras, M. R. Pino, and R. Mittra, "Solution of Electrically Large Problems with Multilevel Characteristic Basis Functions," *IEEE Transactions on Antennas and Propagation*, **AP-57**, 10, October 2009, pp. 3189-3198.
28. S. Rao, D. Wilton, and A. Glisson, "Electromagnetic Scattering by Surfaces of Arbitrary Shape," *IEEE Transactions on Antennas and Propagation*, **AP-30**, 3, May 1982, pp. 409-418.
29. R. Maaskant, *Analysis of Large Antenna Systems*, PhD dissertation, Eindhoven University of Technology, Eindhoven, 2010.
30. R. F. Harrington, *Field Computation by Moment Methods*, New York, Macmillan Company, 1968.
31. G. H. Golub and C. F. van Loan, *Matrix Computation*, Baltimore, MD, John Hopkins University Press, 1989.
32. C. Delgado, F. Catedra, and R. Mittra, "A Numerically Efficient Technique for Orthogonalizing the Basis Functions Arising in the Solution of Electromagnetic Scattering Problems Using CBFM," IEEE International Symposium on Antennas and Propagation, Honolulu, Hawaii, June 2007, pp. 3608-3611.
33. D. H. Schaubert, and A. O. Boryssenko, "Subarrays of Vivaldi Antennas for Very Large Apertures," Proceedings of the 34th European Microwave Conference, Amsterdam, 2004, pp. 1533-1536.
34. D. H. Schaubert, S. Kasturi, M. W. Elsallal, and W. van Cappellen, "Wide Bandwidth Vivaldi Antenna Arrays – Some Recent Developments," Proceedings of the European Conference on Antennas and Propagation, Nice, France, 2006.